

From deterministic dynamics to kinetic phenomena

S. Denisov, A. Filippov, J. Klafter, and M. Urbakh

School of Chemistry, Raymond and Beverley Sackler Faculty of Exact Sciences, Tel-Aviv University, Tel-Aviv 69978, Israel

(Received 11 November 2003; published 29 April 2004)

We investigate a one-dimensional Hamiltonian system that describes a system of particles interacting through short-range repulsive potentials. Depending on the particle mean energy ϵ the system demonstrates a spectrum of kinetic regimes, characterized by their transport properties ranging from ballistic motion to localized oscillations through anomalous diffusion regimes. We establish relationships between the observed kinetic regimes and the “thermodynamic” states of the system. The nature of heat conduction in the proposed model is discussed.

DOI: 10.1103/PhysRevE.69.042101

PACS number(s): 05.40.-a, 05.45.Pq, 05.90.+m, 05.60.Cd

The question of how statistical laws emerge from microscopic dynamics has been a subject of interest for a long time [1]. Studies of relatively simple dynamical systems provide a link between deterministic dynamics and diffusion phenomena [2,3]. In particular, a number of recent dynamical models aim at understanding the necessary and sufficient conditions for a system to obey the Fourier heat conduction law [4]. These examples cover only a part of general problem of how kinetic and thermodynamic properties emerge from dynamics at the atomic scale.

In this paper we propose a many-particle Hamiltonian model which exhibits a wide range of mass and energy transport regimes, and allows to establish relationships between microscopic properties and thermodynamical and kinetic phenomena. We demonstrate that kinetic properties of the system are determined by one controlling parameter, which is a mean energy per a particle, ϵ . Varying ϵ one can cover the whole spectrum of diffusion regimes, from ballistic motion to “frozen” states through anomalous diffusion regimes. We show that the observed kinetic regimes are strongly related to the “thermodynamic” states of the system which change from a “solid” to “gas” phase as the parameter ϵ increases.

The model describes a system of N classical particles each characterized by coordinate x_i and the conjugate momentum p_i . The particles interact through a repulsive short-range potential according to the following Hamiltonian:

$$H(x_i, p_i) = \sum_{i=1}^N \frac{p_i^2}{2} + \frac{A}{2} \sum_{i,j=1}^N e^{[-(x_i-x_j)^2/\sigma^2]}, \quad (1)$$

where A is the strength of interparticle interaction and σ is the width of repulsive core. The particles are located on an interval of length L , and periodic boundary conditions are applied. The mean energy and density of particles are defined as $\epsilon = E/N$ and $\rho = N/L$, respectively, and the mass of particles $m = 1$. Although Eq. (1) describes a one-dimensional system of particles we allow the possibility that the particles can pass through each other. This leads to a spectrum of dynamical behaviors and mimics higher dimensions. Without assuming particle’s transparency the model reduces to the standard picture discussed in textbooks.

In the high-energy limit $\epsilon/A \gg 1$, the system in Eq. (1) behaves as a gas of freely flying particles, slightly perturbed

by weak interactions. In the opposite low-energy limit $\epsilon/A \ll 1$, the system forms a crystal lattice with a constant $a_0 = 1/\rho$. In this solidlike state each particle oscillates at the minimum of potential well formed by its neighbors. In the gas phase the system is uniform while in the solid state it has a discrete translational symmetry with a lattice constant a_0 . According to Kolmogorov-Arnol’d-Moser theorem, in both limits, the system exhibits an ordered dynamical behavior in a region of positive measure in phase space [6]. Due to a difference in symmetries of the ordered states one can expect that a transition between these two states with the change of ϵ will occur through a mixed disordered state.

To study the dynamics of the system in Eq. (1) we use the following algorithm: At the beginning we put all particles at an equal distance a_0 from each other and give them a kinetic energy according to the Maxwell distribution. After that we rescale velocities of the particles in order to get a total energy equal to $N\epsilon$. Then, for each time step, we integrate the corresponding dynamical equations using a central difference symplectic scheme [5]. To extract an information on the structure and dynamics we introduce also a sorted array of particles, $\{x_j^{sort}(t)\}$, where particles are renumbered according their actual instantaneous position, $\{j\} = \text{sort}(\{i\})$.

In order to illustrate a nature of excitations in the system we show in Fig. 1(a) a time evolution of energy distribution initiated by a local perturbation at time $t=0$ that had a form of a kicked group of a few central particles. Here particles with high and low instantaneous velocities are displayed by light and dark colors, respectively. The light regions are organized into lines which correspond to excitations propagating along the system. Three types of excitations with different group velocities, which are given by an inverse slope of the lines, can be distinguished: flying particles, low-energy phonons, and nonlinear solitonic excitations which are intermediate in energy between them. The first dynamical mode, flying particles, dominates in the gas state, $\epsilon/A \gg 1$. Nonlinear excitations and phonons play the main role in the opposite solid-state limit $\epsilon/A \ll 1$ [Fig. 1(c)]. An energy exchange between different modes is most effective in a “liquidlike” state, which corresponds to $\epsilon/A \approx 1$. Interactions between modes can lead, for example, to a transformation of flying particle into solitonic excitation [see the circle in Fig. 1(a)] or to “burning” of flying particle from a sea of phonons and nonlinear excitations [see the circle in Fig. 1(b)].

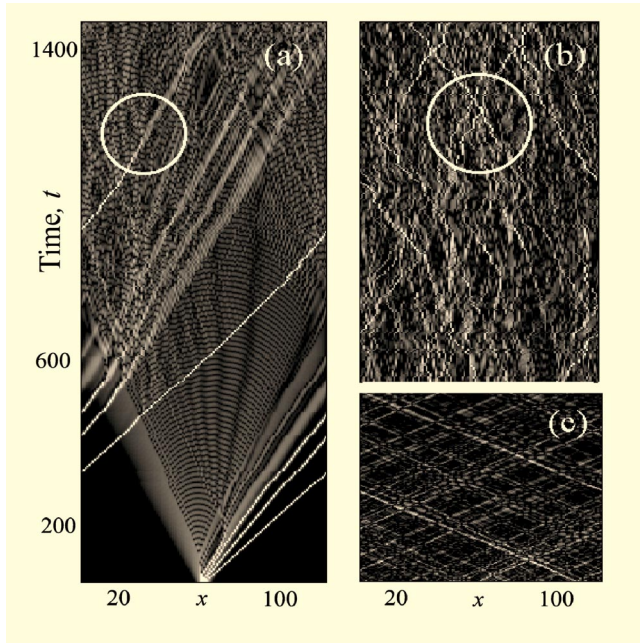


FIG. 1. (a) Time evolution of the energy distribution initiated by kicking of few central particles, for the system in Eq. (1) ($N = 128, \epsilon/A = 0.25$). The circle indicates a collapse of flying particle into a nonlinear excitation. (b) The same system after time $t = 5000$. The circle indicates a birth of two flying particles from the excitation sea. (c) The set of propagating solitons for the system in Eq. (1) for $\epsilon/A = 1$.

In order to describe quantitatively a structure of different “thermodynamic” states arising in the system, we introduce a reduced distance for a sorted set of particles, $\xi_j = [x_j^{sort}(t) - x_{j-1}^{sort}(t) - a_0]$, and calculate the probability density function (PDF) $\Phi(\xi)$, $-a_0 < \xi < L/2$ (see Fig. 2). In the low-energy limit the PDF $\Phi(\xi)$ is governed by a peak near the point $\xi = 0$, which corresponds to a crystal lattice (a right inset in Fig. 2). In the gas limit the PDF scales as (see left inset in Fig. 2)

$$\Phi(\xi) \sim e^{-\chi(\xi - a_0)}. \quad (2)$$

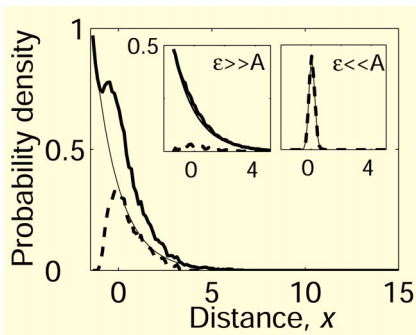


FIG. 2. The PDF $\Phi(\xi)$ calculated for the liquid state, $N = 64$, $A = 1$, $\epsilon = 0.25$, $\rho = 1$, $\sigma = 1$. The thin line shows fitting to $\Phi_{gas}(\xi)$ in Eq. (2). Dashed line corresponds to $\Phi_{solid}(\xi) = 1 - \Phi_{gas}(\xi)$. Left inset shows PDF $\Phi(\xi)$ in gas state ($\epsilon/A = 10$) and the right inset corresponds to solid state ($\epsilon/A = 0.1$).

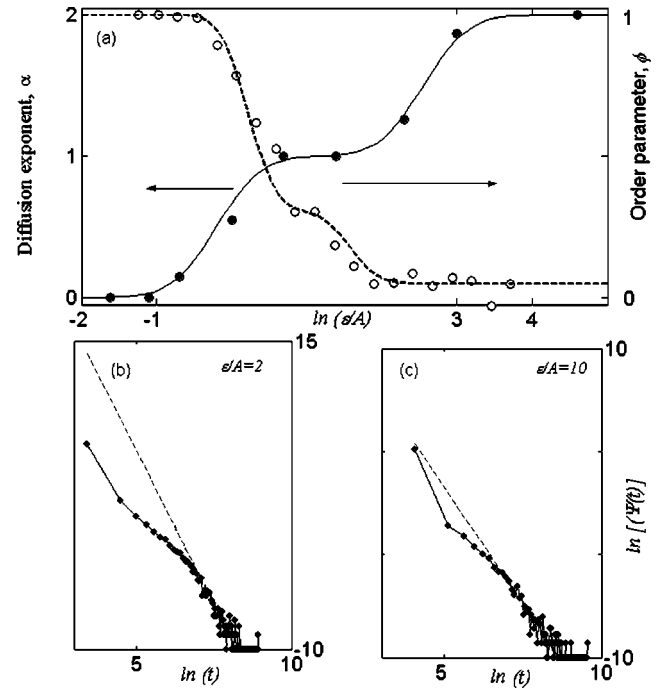


FIG. 3. (a) The dependence of the order parameter, Eq. (4), ϕ (black circles) and the diffusion exponent α , Eq. (5) (open circles), obtained by fitting of the mean squared displacement, $\langle x^2(t) \rangle$, for a calculation time $t = 10^4$; The histograms for a duration of a single flight, $\Psi_{fl}(t)$, for (b) $\epsilon/A = 2$ and (c) $\epsilon/A = 10$; $N = 512$. Uncertainty in α in the intermediate range is about 10%.

It is natural to assume that in the intermediate, liquid state the PDF $\Phi(\xi)$ can be presented in the form

$$\Phi(\xi) = \Phi_{solid}(\xi) + \Phi_{gas}(\xi), \quad (3)$$

where $\Phi_{solid}(\xi)$ (a dashed line in Fig. 2) and $\Phi_{gas}(\xi)$ (a thin line in Fig. 2) describe a solid-state and gas contributions correspondingly. The solid and gas contributions can be isolated from the net PDF by fitting its asymptotics to the exponential distribution, Eq. (2), at negative and large positive ξ . Then Eq. (3) allows to introduce the order parameter, which presents a fraction of solid phase

$$\phi = \frac{\int_{-a_0}^{L/2} \Phi_{solid}(\xi) d\xi}{\int_{-a_0}^{L/2} \Phi(\xi) d\xi}. \quad (4)$$

Figure 3(a) shows a dependence of the order parameter ϕ on the energy density ϵ . It exhibits a phase transition from the gas to solid state as ϵ/A decreases. The plateau at $\epsilon/A \approx 1$ indicates the presence of the third, mixed state that can be associated with a liquidlike phase. Below we consider regimes of mass and energy transfer which correspond to the different thermodynamic states.

Flying particles. Particles can fly only when their velocities are higher than a threshold value, $v_{fl} \approx \sqrt{2U_{max}}$, which is determined by the height of the effective potential created by neighboring particles. The latter can be estimated as a

barrier in a periodic lattice, formed by particles in the solid state, $U_{max} \approx A\{1/2 - \exp[-(a_0/\sigma)^2]\}$.

Each particle dynamics can be characterized by the mean squared displacement $\langle x^2(t) \rangle$, which in the long-time limit follows

$$\langle x^2(t) \rangle \sim t^\alpha, \quad (5)$$

where $\alpha=1$ for normal diffusion. All processes with $\alpha \neq 1$ are known as anomalous diffusion [7,8], being subdiffusion for $0 < \alpha < 1$ and superdiffusion for $1 < \alpha < 2$.

The numerical results presented in Fig. 3(a) clearly show three different dynamical regimes.

(1) Absence of diffusion for $\epsilon/A \ll 1$ (solid phase). In this case particles perform small oscillations around the minima of the potential, and as a result $\alpha=0$.

(2) A ballistic regime with $\alpha=2$ for $\epsilon/A \gg 1$ (gas phase).

(3) Normal diffusion $\alpha=1$ in the liquidlike state where $\epsilon/A \sim 1$.

It should be noted that the latter regime exists for a finite interval of ϵ . For the values of ϵ corresponding to gas-liquid and liquid-solid transitions we have found regimes of anomalous diffusion, namely a superdiffusion in the first case and subdiffusion the second case (Fig. 3) [9].

In the case of superdiffusion each particle performs both flights and trapped oscillations, randomly switching between these two dynamical modes [see Figs. 1(a) and 1(b)]. We have obtained the histogram for a single flight time $\Psi_{fl}(t)$, accumulating the lifetime and length during the interval where the sign of the particle velocity is fixed. It shows an asymptotic power law decay [Fig. 3(b)] $\Psi_{fl}(t) \sim t^{-\gamma}$, with the exponent $\gamma \approx 2.5$ for the gas phase ($\epsilon/A=10$) that corresponds to superdiffusion and $\gamma \approx 3$ for the high-energy edge of the liquid phase, at $\epsilon/A=2$, that corresponds to a transition to normal diffusion regime. The related PDF has the same power behavior. We note that the flying particles do not have a constant velocity.

The subdiffusion, which has been found in the transition region between solid and liquid states, corresponds to short random jumps of the particles interrupted by long trapping events. At low energies the probability of strong fluctuations which can result in a particle escape from the potential well becomes very low. This leads to anomalously long trapping of particles. The particle motion becomes subdiffusive when the PDF of trapping times has a power law asymptotic $\Psi_{tr}(t) \sim t^{-1-\beta}$ with $\beta < 1$ [8]. In this case the diffusion exponent α in Eq. (5) equals β , $\alpha = \beta < 1$. The subdiffusive dynamics can be quantitatively described using a continuous-time random walk approach [8]. It should be noted that flying events are expected in all dynamical regimes. However, what distinguishes among phases are the distributions of flight times or segments.

Solitary excitations and phonons. In the low-energy regime the system tends to build a crystal-type structure. Local energy fluctuations can create here only relatively smooth nonlinear excitations as well as small-amplitude phonons. In the phonon state particles are mainly localized in the middle point between two nearest neighbors, and the variable ξ_j introduced earlier can be used as a small parameter, ξ_j/a_0

$\ll 1$ [11]. Linearization of the equations of motion for the Hamiltonian in Eq. (1) gives the elastic constant $C = (2A/\sigma^2)[1 - 2/(\sigma\varrho)^2]e^{-1/(\sigma\varrho)^2}$, which contains all information on the phonon spectrum [11]. This approximation is not valid for nonlinear excitations, where particles can strongly deviate from their equilibrium positions. However, in the case of smooth excitations the displacements of particles with respect to the corresponding middle points change slowly with particle number j in the sorted array x_j^{sort} , and the difference $y_j = (x_{j+1}^{sort} + x_{j-1}^{sort})/2 - x_j^{sort}$ can be considered as a smooth variable $y = y(x, t)$. One can rewrite the Hamiltonian in Eq. (1) in terms of the continuous variable $y(x, t)$ and prove that the solitonic nonlinear excitations propagating with a constant velocity $y = y(x - vt)$ indeed exist in the system.

We have found that such solutions exist only for particle densities which are below a critical density $\varrho_{crit} = 1/a_{0crit} = \sqrt{2}/\sigma$. For the densities higher than the critical one the width of the excitations reduces to a single-particle scale and the smooth nonlinear excitations cannot exist. Under this condition the liquid state [the plateau in Fig. 3(a)] almost disappears and a transition between solid and gas phases goes directly through a ‘‘sublimation’’ process. Numerical studies of the nonlinear solutions show that they have properties of ‘‘quasiparticles.’’ They propagate in both directions practically without a loss of energy [see Fig. 1(c)] and collide with each other. Interactions between different types of excitations produce an intensive energy exchange in the liquid state that leads to the most efficient thermalization of the system in this state.

Heat conduction. The proposed system provides a possibility to simulate kinetic properties of classical low-dimension systems [4]. As an example we consider a problem of heat conductivity. For this purpose the system in Eq. (1) is coupled to the heat reservoirs placed at the walls $x=0$ and $x=L$. The temperatures at the left and the right walls are given by T_l and T_r ($T_l > T_r$), respectively. When a particle collides with a wall at temperature $T_{l,r}$, it is reflected back with a velocity chosen from the distribution $f(v) = (|v|/T_{l,r}) \exp(-mv^2/T_{l,r})$. To calculate a temperature profile we evaluate time averages as follows: we divide the interval L into a set of equal cells, X_s , $s=1, N-1$, with a length $\Delta X = L/N$. In Fig. 4 we show the local temperature distribution $T(x) = \langle v_s^2 \rangle / 2$ found for different thermodynamic phases of the system in Eq. (1). Here $\langle v_s^2 \rangle / 2$ is an average kinetic energy of the s cell and $\langle \rangle$ denotes a time averaging. s denotes the location along the interval and corresponds in a continuum description to x . In the gas limit the temperature profile exhibits a wide plateau which is typical for a ballistic mechanism of conductivity (Fig. 4, open circles). In this case the heat transfer is determined by flying particles. In the opposite, solid-state, limit we also find ballistic conductivity which is determined by propagating quasiparticles: solitonic excitations and phonons (Fig. 4, open circles) [4]. In the liquid state the $T(x)$ has a strong nonlinear profile with a substantial nonzero slope that is a result of intensive scattering processes and energy exchange between all dynamical modes (Fig. 4, filled circles). The local density of particles,

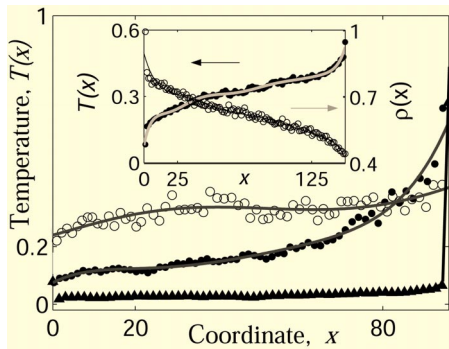


FIG. 4. Local temperature profiles T_i for $\epsilon/A=10$ (open circles), $\epsilon/A=1$ (filled circles), and $\epsilon/A=0.1$ (triangles); $N=100$, $T_l=2$, $T_r=0.1$. Inset shows local temperature profile and local density of particle, calculated for $T_l=0.1, T_r=2$, $N=128$, $\epsilon/A=0.25$. Lines obtained by averaging over 100 realizations after a transient time $t=10^4$.

$\rho(x)=\langle n_s \rangle/N$, where n_s is the average number of particles per cell, also demonstrates a nonlinear profile, which is complimentary to the temperature profile. The observed variation of $\rho(x)$ can be explained by an accumulation of slow particles at the cold end and by fast escape of flying particles from the hot end. A relation between temperature and concentration gradients, which is usually assumed for a macro-

scopic system close to equilibrium, naturally emerges from the proposed Hamiltonian model.

Our calculations show that the proposed system can be used as a model for *thermoengine* that transforms heat into a directed motion. For this purpose the ensemble of particles should be coupled to a third body, i.e., a cargo. Slow particles moving from the cold end affect the cargo stronger than fast particles that move from the hot end. This asymmetry leads to a directed motion of the cargo. Another example of transformation of thermal energy into a directed motion is a production of *electric current* due to temperature differences of thermostats. To simulate this phenomenon we have considered two kinds of particles with different masses and opposite charges. When the difference in the masses of the particles is large enough the light ones can fly ballistically and transfer current while the heavy ones remain immobile.

In summary we have introduced a simple dynamical model that establishes the relationships between microscopic properties of Hamiltonian systems and “macroscopic” thermodynamical and kinetic phenomena. Depending on the energy the model exhibits three well-defined states and a wide spectrum of kinetic phenomena.

Financial support for this work by grants from the Israel Science Foundation (Grant No. 573/00) and BSF is gratefully acknowledged.

-
- [1] P. Ehrenfest and T. Ehrenfest, *The Conceptual Foundations of the Statistical Approach in Mechanics* (Cornell University Press, Ithaca, NY, 1959); N. S. Krylov, *Works on the Foundation of Statistical Physics* (Princeton University Press, Princeton, NJ, 1979).
- [2] S. Grossmann and H. Fujisaka, Phys. Rev. A **26**, 1779 (1982); T. Geisel and J. Nierwetberg, Phys. Rev. Lett. **48**, 7 (1982).
- [3] J. Klafter and G. Zumofen, Phys. Rev. E **49**, 4873 (1994).
- [4] S. Lepri, R. Livi, and A. Politi, Phys. Rep. **377**, 1 (2003).
- [5] J. M. Hail, *Molecular Dynamics Simulation: Elementary Methods* (Wiley, New York, 1992).
- [6] G. M. Zaslavsky, *Physics of Chaos in Hamiltonian Dynamics* (Imperial College Press, London, 1998).
- [7] M.F. Shlesinger, G.M. Zaslavsky, and J. Klafter, Nature (London) **363**, 31 (1993); J. Klafter, M.F. Shlesinger, and G. Zumofen, Phys. Today **49**(2), 33 (1996).
- [8] G. Zumofen and J. Klafter, Phys. Rev. E **51**, 1818 (1995).
- [9] It should be noted that phases discussed above present long-lived out-of-equilibrium states. After a crossover time $t_c \sim 10^5$, the exponent changes to $\alpha=1$ (normal diffusion). We have found that the transient time increases with N and the out-of-equilibrium states become stationary solutions for $N \rightarrow \infty$. The link between relaxation to equilibrium and anomalous diffusive motion in classical N -particle Hamiltonian systems with energy conservation have been discussed in Ref. [10].
- [10] V. Latora, A. Rapisarda, and S. Ruffo, Phys. Rev. Lett. **83**, 2104 (1999).
- [11] A. M. Kosevich, *The Crystal Lattice: Phonons, Solitons, Dislocation* (Wiley-VCH, Berlin, 1999).